Correlation between field-test and laboratory results for a Proton Exchange Membrane Fuel Cell (PEMFC) used as a residential cogeneration system

Nicolas PAULUS[1*], Camila DAVILA[1], Vincent LEMORT[1]

[1]University of Liège, Thermodynamics Laboratory, Liège (Belgium)
[*](Corresponding author: nicolas.paulus@uliege.be)

Abstract – This correlation work is mainly based on a field-test empirical efficiency model developed in a parallel study [1]. Another previous research work has studied laboratory steady-state performance of the same system [2] but those are very different than real field-test applications because the in-situ operating conditions are specific to the installation, the climate and the occupant's behavior. Despite that, this work demonstrates how a correlation can still be conducted, mainly by implementing a primary energy penalty on the steady-state nonrealistic laboratory results.

Nomenclature

cp	specific heat capacity of water, J.kg^{-1}.K^{-1}
C_γ	minimum value for the γ_1 correction factor applicable to the dataset of laboratory results for field-test correlation, -
DHW	Domestic Hot Water
$\dot{m}$	water flow rate, kg.s^{-1}
HHV	High Heating Value, kWh.m^{-3}
LHV	Low Heating Value, kWh.m^{-3}
$Max_{\overline{T_{R,4h}}}$	maximum value of $\overline{T_{R,4h}}$ for the whole dataset, -
Q_{DHW}	monitored heat produced by the machine for DHW production, kWh
Q_{SH}	monitored heat produced by the machine for space heating, kWh
$\overline{T_{R,4h}}$	non-dimensionalized daily maximum 4h gliding average temperature of the return, -
$(Q_{SH}+Q_{DHW})_{aj}$	adjusted total heat demands of the day (with correction factor γ_1), kWh
$\dot{V}_{gas}$	gas volume flow rate consumption, m^3.s^{-1}

Greek symbols

η_{th}	LHV thermal efficiency
$\gamma_{1,2}$	correction factors to account for working temperature levels (1) and unsmooth heat demands (2), -
ΔT	temperature difference between depart and return of space heating appliance, K
φ_0	primary energy penalty applied to laboratory testing to allow correlation with field-test model, kWh

1. Introduction

This work takes into account two previous studies on which it bases its correlation. The first one, a field-test study of two systems implemented in Belgium houses in 2020, has built daily performance models of the machine [1], which consists of a residential gas boiler hybridized to a PEMFC and therefore aims to help reaching the global warming goals sets in the "Paris Agreement" [3]. One of those models is slightly adapted in this work. The other one is a purely laboratory study [2] that provided, amongst other interesting results, steady-state figures that serve as a base for this work. As this one, all those previous studies consider identical machines whose expected performance and schematics are respectively reported in Table 1 and Figure 1. One particularity of the system is that it requires a fuel cell shutdown recovery procedure of 2.5 hours at least every two days to handle reversible ageing PEMFC processes [4].

1.1. Field-test - description of the monitored houses and the space heating architecture

The first house is located in Huy (South-East of Belgium) whereas the other one is located in Oostmalle (North of Belgium). The same climatic region can be assumed for the two houses.

The first monitored building (Huy) is a semi-detached house of the early 20th century but significant insulation work of walls and roofs has been conducted. Single-glazing windows have been replaced by double-glazing windows and a balanced ventilation has been installed. However, terminal units still consist of high temperature radiators. The family that lives there consists of 2 active adults and 3 children under the age of 10.

Datasheet figures	*Values*
Maximum electrical production a day	17 kW_{el}
Fuel cell rated electrical & thermal power	0.75 kW_{el} & 1.1 kW_{th}
Electrical LHV efficiency of the PEMFC	37 %
Max global Fuel cell LHV efficiency	92 %
Max LHV boiler efficiency (at rated power)[a]	108.6 %

[a] Considering HHV to LHV ratio of 1.1085 *[5]*

Table 1: *PEMFC gas boiler hybrid expected targets (data provided by manufacturer)*

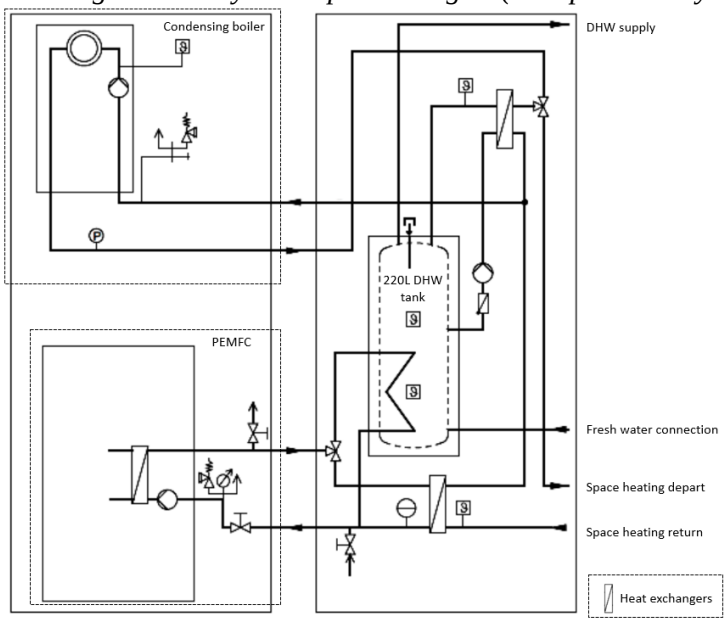

Figure 1: *Hybridization's architecture of the PEMFC with the gas condensing boiler and the DHW tank*

The second monitored building (Oostmalle) is a fully detached house from the 70s but deep renovation has just taken place before the study. Insulation of course, but the whole space heating architecture has also been revisited with the implementation of floor heating for the ground floor. On the first floor, terminal units consist of high temperature radiators. The family involves a young active couple and one child of small age.

1.2. Field-test - Acquisition chain (from the monitoring sensors to the cloud)

Both houses are equally monitored according to the scheme of Figure 2. Sensor reference, precision and resolution of the acquired data are presented in Table 2. Monitoring sampling rate has been set to a 2-minute or a 5-minute time step, respectively for Huy and Oostmalle [6].

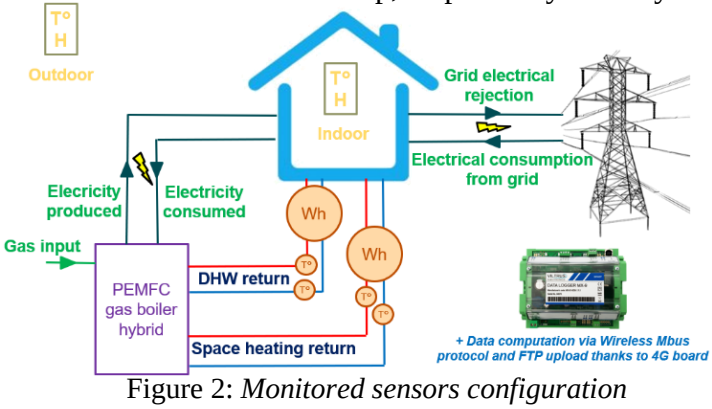

Figure 2: *Monitored sensors configuration*

1.3. Field-test - Resulting model

The field-test model reused in this work provides the daily LHV thermal and electrical efficiencies [1]. It is worth mentioning that electrical consumption of the auxiliaries (for example, the circulator) is not taken into account in the efficiency calculations, mainly because a net electrical consumption of the system only occurs when the PEMFC is not producing [6], which is one of the reasons why the electrical consumption of the unit is not that significant [7].

Sensors	*Reference*	*Accuracy*
Temperature and humidity	Weptech Munia	± 0.3 K | ± 2 %
DHW and space heating heat counters	Qalcosonic E1 Qn2,5 qi=0.025m³/h | L=130mm	Accuracy Class 2 [8]
Machine & house 2-ways electrical energy counter	Iskraemeco MT174-D2A42-V12G22-M3K0	Accuracy Class 1 [9]
Gas volume counter	BK-G4T DN25 Qmax 6 m³/h	<0.5%

Table 2: *Reference of the monitoring sensors. Data logger (cloud connection) is a Viltrus MX-9*

The field-test models offered a good fit despite the fact that the two installations are pretty different as far as the owner's heat demands are concerned [1]. The chosen model (and its goodness of fit) is presented in Figure 3. It takes as inputs the daily total heat demand ($Q_{SH} + Q_{DHW}$) and the daily electrical production of the unit (or its daily load factor [1]). It also implements two correction factors (γ_1 and γ_2) in order to take into account two physical sensitivities that have an impact on the resulting efficiency (and it therefore provides a better fit). The first effect that is taken into account is that higher working temperatures decrease the thermal efficiency (for identical heat demands). This has also been stated for other heating devices in literature [10]. Thus, considering as a first approach that the relation between thermal efficiency and total heat demand is linear (for a given heat demand window), one has concluded that the monitoring data (in this case, the total heat demand) can be adjusted linearly with a first non-dimensionalized correction factor γ_1 as proposed with equation (1) and equation (2) [1]:

$$(Q_{SH} + Q_{DHW})_{aj} = (Q_{SH} + Q_{DHW}) \times \gamma_1 \quad (1)$$

Where:

$$\gamma_1 = 1 - \frac{\overline{T_{R,4h}}}{Max_{\overline{T_{R,4h}}}} \times 0.3 \quad (2)$$

$\overline{T_{R,4h}}$ is a parameter chosen to be the image of the delivery temperature conditions of the day. The problem is that the machine does not work in steady-state operations for the whole day. Looking only at the maximum temperature of the day in the return line would therefore not be representative and might account for one single (very high) transient effect. Considering the average temperature of the whole day for $\overline{T_{R,4h}}$ is not ideal as well because a very erratic and high temperature space heating demand could result in the same average temperature as the one of a 24h-long low temperature demand (typical of floor heating). Therefore, it has been chosen to look at the return temperature 4h gliding average of the day and keep its maximum value. On the other hand, $Max_{\overline{T_{R,4h}}}$ is the maximum value of $\overline{T_{R,4h}}$ for the whole dataset (both monitored houses and the 365 days considered) [1]. It is worth mentioning that one has only considered the return line temperature, as in literature [10]. Also, in this case, only the space heating is considered for $\overline{T_{R,4h}}$ mostly because DHW production goes mainly into the tank and is not directly monitored (see Figure 1).

The second effect the chosen model is considering is that possible erratic behavior (highly transient) tends to decrease the thermal efficiency, as seen in literature [11]. The chosen model establishes a second correction factor γ_2 to that end [1] but it will not be used in this paper because the laboratory conditions used for the correlation are steady-state only [2].

The empirical model is a polynomial regression of the third order on both dimensions and is defined by equation (3) (x being the total adjusted total heat demands from equation (1) and y being the daily electrical production). Parameters models of equation (3) are shown in Table 3.

$$f(x,y) = p_{00} + p_{10}x + p_{01}y + p_{20}x^2 + p_{11}xy + p_{02}y^2 + p_{30}x^3 + p_{03}y^3 + p_{21}x^2y + p_{12}y^2x \quad (3)$$

p_{00}	p_{01}	p_{10}	p_{02}	p_{11}	p_{20}	p_{03}	p_{12}	p_{21}	p_{30}
24.27	-1.648	3.024	0.01102	-0.01704	-0.04291	$7.329e^{-5}$	$6.384e^{-4}$	$1.597e^{-4}$	$1.976e^{-4}$

Table 3: *Values for the parameters of the field-test model of equation (3)*

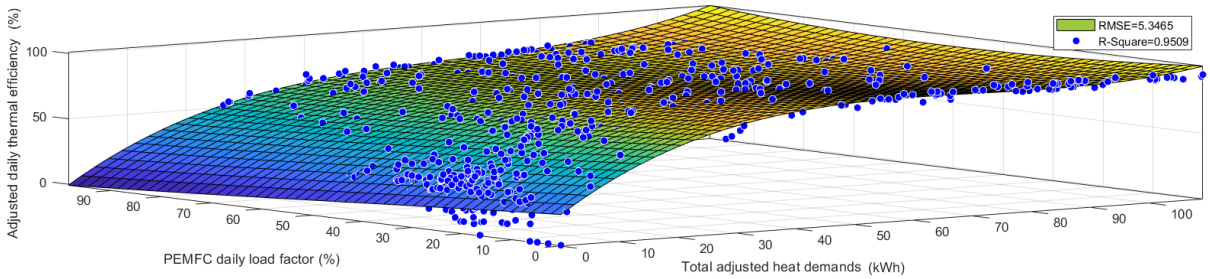

Figure 3: *Resulting LHV efficiency model from the field-test monitoring study [1].*

1.4. Laboratory steady-state tests

The schematics [2] of the test bench for the steady-state experiments is shown in Figure 5. To prevent warranty loss, the measurements inside the modules could not be invasive; only surface thermocouples were installed on the pipes around and in the machine. Only the *W3* water meter could be placed in the system itself thanks to proper intended hydraulic interfaces.

The test bench principle was for the heat demand to be emulated by an auxiliary heat exchanger (*Heat ex.* on Figure 5), whose capacity is controlled by a ball valve *V2* that regulates the water flow on the cold side. The demand of DHW is controlled by adjusting the opening of another ball valve *V1* at the outlet of the system. The *V3* valve on the gas inlet is only there for security reasons and shall not be altered. All the sensors of the test bench are represented in Figure 5. For increased representativity of enthalpy measurements [12], in-pipe thermocouples (facing incoming fluid) were placed thanks to manufactured immersion sleeves (as shown in Figure 4). Type of sensors are presented in Table 4 along with their accuracy.

Based on the EN 50465, four main test campaigns were performed: one with only the DHW valve fully opened, one with only the DHW valve 50% opened (the space heating valve being fully closed for both), one with only the space heating valve fully opened and at last one with only the space heating valve 50% opened (the DHW valve being fully closed for both) [2]. The results of those campaigns have been reproduced in Table 5 and Table 6. The HHV values have been given by the gas provider [2] and HHV to LHV ratio has been assumed to be 1.1085 [5]. The LHV equivalent energy of the gas has been computed considering the difference between delivery (about 1 atm, about 288.15 K) and HHV measurements standard conditions (1 atm, 273.15K) [1]. Measured thermal energy assumes a constant calorific value *cp* of 4184 J/kg-K (assumption similar to initial work [2]). Thermal LHV efficiency can thus be trivially obtained. Electrical efficiency is not shown because the output electrical power has been verified to be quite constant and equal to the targeted 750 W (of Table 1) [1].

Sensor	*Type*	*Accuracy*	*Number of measure points*
Thermocouples	T	± 0.3 K	24
Water meter	Volumetric	± 2 % Q_n ; ± 5% Q_{min}	3
Gas meter	Diaphragm	± 0.5 %	1
Power meter	Multifunctional	± 0.5 %	1

Table 4: *Laboratory test measurement devices specifications*

Figure 4: *Thermocouples immersion sleeves: surface and elbow thermocouples*

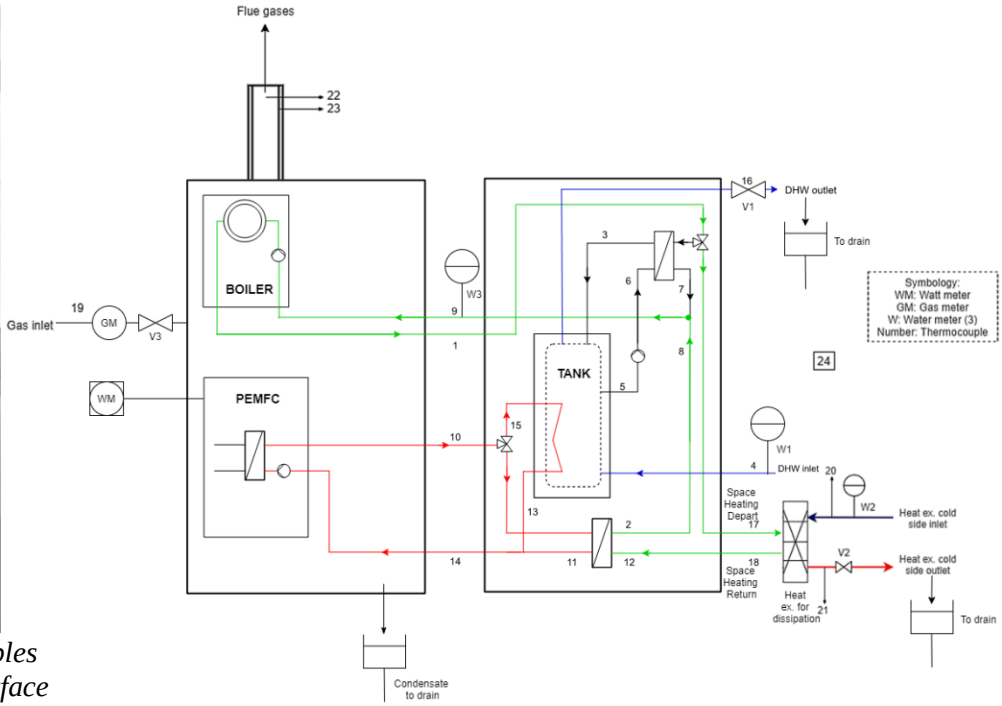

Figure 5: *Complete schematics of the test bench*

2. Correlation

It is clear that the best way to operate a correlation would have been to reproduce one typical day seen on the field-test in a laboratory but this could not be done. Laboratory operating conditions and field-test are thus difficult to correlate because the whole field-test analyses have been established based on daily values (not close at all from the laboratory steady-state operating conditions). In addition, the laboratory tests have been conducted for about 45 minutes only and do not include the warming up of the tank. Also, there is pretty much no standby losses in those laboratory tests as the heat demand is always there and the 3-way valves (Figure 1) are mainly switched to bypass the tank so the heat is directly measured by the sensors at the outlets. For DHW tests, the tank is not bypassed but there is still pretty much no storage effect as the enthalpy flow that comes in also comes out (so the standby losses are also insignificant).

On the other hand, in the field-test, standby losses are not negligeable, especially in low heat demand days (which account for similar heating demands as the 45-min laboratory tests, i.e. lower than 25 kWh as seen in Table 5 and Table 6). Therefore, a compensation parameter shall be applied on the laboratory results to ensure relevancy with the field-test model.

It is performed by considering a fictive extra primary energy consumption (or primary energy penalty) φ_0 at the denominator of the "adjusted" efficiency formula of the laboratory tests, presented in equation (4).

$$\text{Adjusted } \eta_{th} = \frac{\int \dot{m} \times cp \times \Delta T \times dt}{\varphi_0 + \int \dot{V}_{gas} \times LHV \times dt} \quad (4)$$

$\int \dot{V}_{gas}$ is the gas consumption, $\int \dot{m}$ is the mass of water heated during the test (relative density assumed to 1), ΔT is the thermal difference between depart and return to the system. All those measurements are given in Table 5 and Table 6. All the terms shall be expressed in kWh (and based on LHV). Optimized penalty φ_0 to be applied to laboratory tests has been set to 10 kWh for fitting reasons. This value happens to be equal to the amount of energy that can be considered to be store in the 220 L DHW tank of the unit (thermally loaded temperature of 60°C compared to 20°C of rest temperature). As a first approach, this lump sum value of 10 kWh can be considered as the daily stand-by losses that are occurring onsite. Since DHW scheduling occurs pretty much every day (up to about 60°C as well), the daily standby losses with this

system can be considered to approximate the total energy that can be stored in the tank. It is worth mentioning that the "Adjusted η_{th}" of the laboratory results has only been computed for correlation purposes and shall not be considered relevant as is (one reason is that higher the working temperature, higher the efficiency, which is against what has previously been stated).

On the other hand, a proper use of the field-test model of equation (3) requires two inputs: x and y. y, the electrical production of the day, can be considered as a first approach as the multiplication of the net power of the PEMFC (observed to be constant and equal to 750 W) by the duration of the test, given in Table 5 and Table 6. x, the adjusted total heat demand of the day, is obtained by multiplying the measured thermal energy (the heat demand, that can directly come from Table 5 and Table 6) to the γ_1 correction factor as described by equation (1).

For the laboratory results, γ_1 can be expressed as a function of a second fitting parameter (C_γ). Indeed, γ_1 accounts for the fact that higher working temperatures tend to decrease the thermal efficiency. Unfortunately, the laboratory data cannot reuse equation (2) as it is designed to be established based on the temperature data of one whole day. However, one can still establish γ_1 manually in a similar way compared to equation (2). Indeed, this equation gives a linear decrease of γ_1 with higher working temperature and this kind of linear behavior can be reproduced for the laboratory tests. The maximum value of γ_1 (which is 1, i.e. no correction) is assumed to be of application with the lowest temperature delivery, which is 20°C (as it can be seen in Table 5 and Table 6). This is coherent because in real operating conditions, heating temperatures shall rarely be lower than 20°C. Maximum operating conditions of 60°C (from Table 5 and Table 6) lead to a minimum value of the γ_1 correction factor, called C_γ (optimized manually to 0.8 for fitting reasons). In fact, by looking at equation (2), γ_1 could reach smaller values (down to 0.7) but it is not advised to assume that the maximum temperature operating conditions of the laboratory tests requires this absolute γ_1 minimum value. Indeed, equation (2) is only valid for the field-test and daily dataset that allows establishing the maximum 4h gliding average of the return temperature. This does not correspond to the laboratory tests operating conditions. Intermediate γ_1 values are subsequently set linearly between 1 and 0.8 (C_γ) according to the working temperature of Table 5 and Table 6.

There is no need to make a difference between the space heating only and the DHW only operating conditions because it has been stated that standby losses and storage effect could be neglected for both laboratory campaigns studied in this work. It can thus be assumed that they can be treated the same way, with the same correction factor (only depending on temperature).

3. Results and conclusions

The correlation method between the chosen field-test model and the laboratory steady-state results for this PEMFC-gas condensing boiler hybrid can be resumed with two main steps.

Firstly, on the one hand, to account for stand-by losses that have not occur in the laboratory steady-state tests, one must apply a primary energy penalty φ_0 on the laboratory results. It has been set equal to 10 kWh, which is equivalent to the amount of thermal energy that can be stored in the 220 L tank of the system. This is an indication of the daily stand-by losses with this system in real applications (with daily DHW scheduling). Thus, one obtains the "Adjusted" LHV thermal efficiency from equation (4), that will be compared to the field-test model.

Secondly, on the other hand, the field-test model of equation (3) intrinsically uses as an input the total heat demand, adjusted (multiplied) with the γ_1 correction factor to account for the effect of the working temperatures on the thermal efficiency of the system. The laboratory measured thermal energy cannot thus be used as is in equation (3) because it has to be multiplied by γ_1, which should therefore be established beforehand. Unfortunately, the method used in the

field-test model study to define γ_1 [1] is not applicable for the laboratory results, but it can be established quite similarly, through optimizing only one fitting parameter, i.e. C_γ.

	Space Heating 100% - DHW 0%												
	Gas Consumption [m3]	Water Consumption [m3]	Mean ΔT° [°C]	Test duration [s]	HHV [kWh/m³]	LHV equivalent gas energy [kWh]	Measured Thermal Energy [kWh]	γ_1 [-]	Adjusted Thermal Energy [kWh]	Electrical Energy [kWh]	Adjusted η_{th} [-]	η_{th} from field-test model [-]	difference between η_{th} [percentage points]
60±1°C	2,4290	1,128	17,205	2693	11,4588	23,628	22,556	0,85	19,172	0,561	0,67	0,67	0,27
50±1°C	2,0100	1,123	14,650	2696	11,4588	19,552	19,121	0,8875	16,970	0,562	0,65	0,63	1,56
40±1°C	1,6400	1,125	12,055	2676	11,4588	15,953	15,762	0,925	14,580	0,558	0,61	0,59	1,91
30±1°C	1,2080	1,137	8,756	2711	11,4588	11,751	11,571	0,9625	11,137	0,565	0,53	0,52	1,32
20±1°C	0,8440	1,144	5,958	2705	11,4588	8,210	7,922	1	7,922	0,564	0,44	0,45	1,13
	DHW Heating 100% - Space Heating 0%												
	Gas Consumption [m3]	Water Consumption [m3]	Mean ΔT° [°C]	Test duration [s]	HHV [kWh/m³]	LHV equivalent gas energy [kWh]	Measured Thermal Energy [kWh]	γ_1 [-]	Adjusted Thermal Energy [kWh]	Electrical Energy [kWh]	Adjusted η_{th} [-]	η_{th} from field-test model [-]	difference between η_{th} [percentage points]
60±2°C	2,3530	0,809	22,913	2718	11,6003	23,171	21,544	0,85	18,312	0,566	0,65	0,65	0,45
55±2°C	2,3990	0,827	23,173	2772	11,6003	23,624	22,273	0,8688	19,350	0,578	0,66	0,67	0,81
50±2°C	2,2490	0,801	22,476	2682	11,6003	22,147	20,924	0,8875	18,570	0,559	0,65	0,66	0,75
45±2°C	1,9360	0,809	19,316	2713	11,6003	19,065	18,162	0,9063	16,459	0,565	0,62	0,62	0,25
40±2°C	1,5930	0,808	16,013	2705	11,6003	15,687	15,037	0,925	13,910	0,564	0,59	0,58	1,02
35±2°C	1,2450	0,800	12,770	2688	11,6003	12,260	11,873	0,9438	11,205	0,560	0,53	0,52	1,31
30±2°C	0,9150	0,788	9,487	2653	11,6003	9,011	8,688	0,9625	8,363	0,553	0,46	0,46	0,01
											Max difference :		**1,91**

Table 5: *Laboratory results [2] (with adjustments) for comparison to field-test model (based on adjusted heat demands with correction factor γ_1 and electrical production) – fully opened heat demand valves*

	Space Heating 50% - DHW 0%												
	Gas Consumption [m3]	Water Consumption [m3]	Mean ΔT° [°C]	Test duration [s]	HHV [kWh/m³]	LHV equivalent gas energy [kWh]	Measured Thermal Energy [kWh]	γ_1 [-]	Adjusted Thermal Energy [kWh]	Electrical Energy [kWh]	Adjusted η_{th} [-]	η_{th} from field-test model [-]	difference between η_{th} [percentage points]
60±1°C	2,3860	0,662	29,204	2678	11,3016	22,891	22,469	0,85	19,099	0,558	0,68	0,67	1,63
50±1°C	2,0010	0,668	24,432	2677	11,3016	19,198	18,968	0,8875	16,834	0,558	0,65	0,63	2,05
40±1°C	1,6530	0,675	20,066	2665	11,3016	15,859	15,742	0,925	14,561	0,555	0,61	0,59	2,09
30±1°C	1,1920	0,678	14,433	2698	11,3016	11,436	11,373	0,9625	10,947	0,562	0,53	0,51	1,58
20±1°C	0,8280	0,68	9,809	2693	11,3016	7,944	7,752	1	7,752	0,561	0,43	0,44	1,04
	DHW Heating 50% - Space Heating 0%												
	Gas Consumption [m3]	Water Consumption [m3]	Mean ΔT° [°C]	Test duration [s]	HHV [kWh/m³]	LHV equivalent gas energy [kWh]	Measured Thermal Energy [kWh]	γ_1 [-]	Adjusted Thermal Energy [kWh]	Electrical Energy [kWh]	Adjusted η_{th} [-]	η_{th} from field-test model [-]	difference between η_{th} [percentage points]
60±2°C	2,0010	0,414	38,253	2728	11,5730	19,659	18,406	0,85	15,645	0,568	0,62	0,61	1,28
55±2°C	1,9240	0,420	36,459	2739	11,5730	18,902	17,797	0,8688	15,461	0,571	0,62	0,60	1,14
50±2°C	1,6120	0,394	32,680	2627	11,5730	15,837	14,965	0,8875	13,281	0,547	0,58	0,56	1,60
45±2°C	1,5360	0,434	28,088	2834	11,5730	15,090	14,168	0,9063	12,839	0,590	0,56	0,55	1,11
40±2°C	1,2070	0,412	23,909	2695	11,5730	11,858	11,448	0,925	10,590	0,561	0,52	0,51	1,67
35±2°C	0,9590	0,415	19,281	2725	11,5730	9,422	9,300	0,9438	8,777	0,568	0,48	0,47	1,25
30±2°C	0,7540	0,414	14,727	2726	11,5730	7,408	7,086	0,9625	6,820	0,568	0,41	0,42	1,26
											Max difference :		**2,09**

Table 6: *Laboratory results [2] (with adjustments) for comparison to field-test model (based on adjusted heat demands with correction factor γ_1 and electrical production) – fully opened heat demand valves*

This fitting parameter C_γ, which is the minimum value of this work for the γ_1 correction factor, is required for the correlation and it has been set equal to 0.8. It is applicable to the laboratory data corresponding to the highest temperature delivery (60°C in this case). Maximum γ_1 value is assumed equal to 1 and relevant for minimum delivery temperature (20°C). The rest of the γ_1 values to apply to the laboratory dataset are set accordingly (linearly between 0.8 and 1). One is thus finally able to fully implement equation (3) with the laboratory measured thermal energy. One subsequently obtains the LHV thermal efficiency from the field-test model, which can be compared to the previously established "Adjusted" laboratory LHV thermal efficiency.

All those manipulations are recorded in Table 5 and Table 6. One can see that the difference between the "adjusted" laboratory efficiency (with the φ_0 penalty) and the field-test model comes down to about 2 percentage point, which is way within the error margin, that can be deduced from the accuracy of the sensors presented in Table 4 (for the laboratory results) and in Table 2 (for the field-test model). For the field-test data, the propagated uncertainty can indeed be established to about ±5%. The method of uncertainty propagation is based on the National Institute of Standards and Technology recommendations and has been fully explained in a parallel field-test study (conducted on another fuel cell cogeneration system) [13].

Even if the two fitting parameters (C_γ, used to establish γ_1 and φ_0 used for adjusting the laboratory results) have manually been optimized, they have still physical meanings. On one hand, C_γ (=0.8) is close to the minimum value allowable for γ_1 of the chosen field-test model (as deduced from equation (2) the minimum γ_1 is 0.7 [1]). On the other hand, φ_0 as already been stated close to the amount of thermal energy storable in the DHW tank of the system.

Such a goodness of fit for all the laboratory data presented in Table 5 and Table 6 is quite amazing. Therefore, it highlights the relevance of the laboratory study [2] but even more significantly of the previous modelling work [1] that provided equation (3), which was actually the main (achieved) purpose of this work. This has been performed despite of the intrinsic differences between laboratory and field-test configurations (for example, big differences in the hydraulic integration and in the sensors that have been used).

References

[1] N. Paulus and V. Lemort, "Field-test performance models of a residential mi-cro-cogeneration system based on a proton exchange membrane fuel cell and a gas condensing boiler," *To be submitted*, 2022.

[2] C. Davila, N. Paulus and V. Lemort, "Experimental investigation of a Micro-CHP unit driven by natural gas for residential buildings," in *Herrick 2022 Proceedings*, Purdue, 2022.

[3] N. Paulus, "Will Greenhouse Gas emission commitments in France and Wallonia respect IPCC's carbon budget ?," *Energy Policy*, Under review, 2022.

[4] N. Paulus and V. Lemort, "Review of probable degradation mechanisms and recovery procedures for reversible performance losses in a residential cogeneration polymer electrolyte membrane fuel cell," To be submitted.

[5] I. Daoud, "Installer une Cogénération dans votre Etablissement," Ministère de la Région wallonne. Direction Générale des Technologies, de la Recherche et de l'Energie (GGTRE), 2003.

[6] N. Paulus, C. Davila and V. Lemort, "Grid-impact factors of field-tested residential Proton Exchange Membrane Fuel Cell systems," in *CLIMA 2022 Proceedings*, Rotterdam, 2022. https://doi.org/10.34641/clima.2022.176

[7] N. Paulus, C. Davila and V. Lemort, "Field-test economic and ecological performance of Proton Exchange Membrane Fuel Cells (PEMFC) used in micro-combined heat and power residential applications (micro-CHP)," in *ECOS 2022 Proceedings*, Copenhagen, 2022.

[8] OIML R 75-, *Heat meters. Part 1*, International Organization of Legal Metrology, 2002.

[9] IEC 62053-21, *Electricity metering equipment (a.c.) – Particular requirements. Part 21 : Static meters for active energy (classes 1 and 2)*, International Electrotechnical Commission, 2003.

[10] S. Baldi, T. Le Quang, O. Holub and P. Endel, "Real-time monitoring energy efficiency and performance degradation of condensing boilers," *Energy Conversion and Management*, vol. 136, pp. 329-339, 2017.

[11] G. Bennett and C. Elwell, "Effect of boiler oversizing on efficiency: a dynamic simulation study," *Building Services Engineering Research and Technology*, vol. 46, no. 6, pp. 709-726, 2020.

[12] P. Klason, G. Kok, N. Pelevic, M. Holmsten, S. Ljungblad and P. Lau, "Measuring temperature in pipe flow with non-homogeneous temperature distribution," *International Journal of Thermophysics*, vol. 35, 2014.

[13] N. Paulus and V. Lemort, "Field-test performance of Solid Oxide Fuel Cells (SOFC) for residential cogeneration applications," in *Herrick 2022 Proceedings*, Purdue, 2022.